Hybrid Reconfigurable Intelligent Surfaces and Unmanned Aerial Vehicle Assisted Communication

Chi Yen Goh[1], Chee Yen Leow[1], Chuan Heng Foh[2], Igbafe Orikumhi[3], and Sunwoo Kim[3]
[1]Wireless Communication Centre, Faculty of Electrical Engineering, Universiti Teknologi Malaysia, Johor, Malaysia.
[2]5GIC&6GIC, Institute for Communication Systems (ICS), University of Surrey, Guildford, U.K.
[3]Department of Electronic Engineering, Hanyang University, Seoul, South Korea.
Email: {yen1997@graduate, bruceleow@}.utm.my, c.foh@surrey.ac.uk, oigbafe2@hanyang.ac.kr, remero@hanyang.ac.kr

***Abstract*—Reconfigurable Intelligent Surfaces (RIS) and Unmanned Aerial Vehicles (UAVs) have emerged as promising technologies for the 6th-Generation (6G) network. The integration of RIS with the UAV (RIS-UAV) can enhance ground communication by providing a 360° panoramic reflection. Existing RIS-UAV mainly considers passive elements which suffer from double path loss problems. This motivates the use of the hybrid RIS-UAV equipped with both active and passive RIS elements. This paper investigates the rate maximisation problem for the hybrid RIS-UAV by optimising the UAV's altitude, transmit power allocation at the base station and hybrid RIS, subject to the hardware power dissipation, transmission power, and flight power. The non-convex joint optimisation problem is addressed using a Genetic Algorithm (GA). The numerical results show that the joint-optimised hybrid RIS-UAV can achieve a rate twice the unoptimised hybrid RIS-UAV and 22 times higher than the conventional passive RIS-UAV.**

***Index Terms*—Reconfigurable intelligent surfaces, UAV, achievable rate, optimisation, wireless communication**

I. Introduction

Reconfigurable intelligent surfaces (RIS) are reconfigurable metasurfaces that are made up of a two-dimensional array of low-cost reflecting elements that can be controlled to manipulate the radio propagation environment [1]. Recently, the integration of RIS with unmanned aerial vehicles (UAV) has emerged as a promising solution to enhance UAV cooperative communication, where the UAVs serve as aerial RIS to assist the communication system. RIS-UAV is the term that refers to the integration of RIS and UAV throughout this paper. By mounting the RIS on the surface of the UAV, the three-dimensional (3D) flexibility and mobility of UAV can be used to provide a 360° panoramic reflection for the incident signals instead of the 180° half-space reflection provided by the conventional terrestrial RIS that are static [2], [3]. Therefore, the RIS-UAV has been widely studied as an aerial RIS to assist the wireless communication system.

However, the existing RIS-UAV mainly consists of passive elements that only reflect the incident signals without modifying them. Thus, the received signals reflected by the passive RIS-UAV experience double path loss problem [4]. To overcome these issues, a hybrid RIS-UAV consisting of both active and passive elements has been introduced [5]. By adding the active load impedance, the hybrid RIS-UAV can amplify the signal while reflecting it towards the desired destination. This approach results in improved signal quality compared to the passive RIS-UAV. Additionally, when compared to the fully active RIS-UAV that demands a larger power budget, the hybrid RIS-UAV emerges as the optimal choice.

There have been several studies on optimising the passive RIS-UAV and the hybrid terrestrial RIS. In [6], [7], UAV trajectory, transmit beamforming at the base station and passive beamforming of the passive RIS were jointly optimised to maximise the average achievable rate and the average secrecy rate of the passive RIS-UAV communication system, respectively. To exploit the advantages of passive RIS and the UAV active relay, [8] studied the integrated passive RIS and UAV active relay system by selecting the transmission mode between the passive RIS-UAV and UAV active relay. Besides, the paper optimised the altitude of the UAV, the number of RIS elements and the transmission mode in order to maximise the system capacity and energy efficiency. By optimising the transmit beamforming at the base station and hybrid terrestrial RIS, [9] demonstrates that the hybrid terrestrial RIS, which utilizes a single active element, achieves an improvement of about 40% in spectral efficiency if compared to the conventional passive terrestrial RIS. Nevertheless, none of the studies consider the optimisation of the hybrid RIS-UAV.

This paper aims to maximise the achievable rate of the hybrid RIS-UAV by optimising the UAV's altitude, transmit power allocation at the base station and hybrid RIS, subject to the power dissipation, transmission power, and flight power consumption. Given the total power, the achievable rate of the optimised hybrid RIS-UAV is analysed and compared to that of the unoptimised hybrid RIS-UAV, as well as the conventional passive RIS-UAV. The numerical results are provided to highlight the potential of the hybrid RIS-UAV.

The paper is organised as follows. In Section II, the system model of the hybrid RIS-UAV is introduced and the rate maximisation problem is formulated. In addition, the algorithm used to solve the optimisation problem is described in that section. Numerical results are presented and discussed in Section III, and conclusions are drawn in Section IV.

II. System Model

As shown in Fig. 1, we consider a downlink communication system assisted by a hybrid RIS-UAV, in which the RIS that is mounted on the rotary-wing UAV, consists of both active and passive reflecting elements. Assuming that the direct link

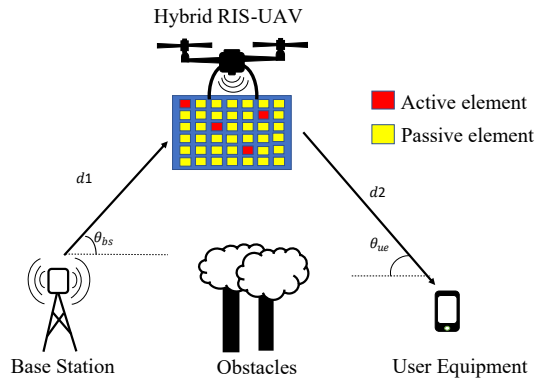

Fig. 1. Hybrid RIS-UAV cooperative communication.

between the base station and the user equipment is blocked, hence the hybrid RIS-UAV serves as a mobile aerial RIS to amplify and reflect the signal from the base station towards the user equipment. While the system focuses on the single-user case, we acknowledge the potential for future research to explore the more general case involving multiple users. For simplicity, both the base station and the user equipment are static and equipped with a single antenna. On the other hand, the hybrid RIS-UAV hovers at a certain altitude while forwarding the signals. Since each of the RIS elements is assumed half of the wavelength size, therefore the signals are reflected with a constant gain from the elements.

The locations of the base station, hybrid RIS-UAV, and the user equipment in 3D Cartesian coordinates are $\boldsymbol{w}_{BS} = (x_{BS}, y_{BS}, 0)$, $\boldsymbol{w}_{UAV} = (x_{UAV}, y_{UAV}, z_{UAV})$, and $\boldsymbol{w}_{UE} = (x_{UE}, y_{UE}, 0)$, respectively. Hence, the distance between the base station and the hybrid RIS-UAV can be computed as:

$$d_1 = \sqrt{\mid \boldsymbol{w}_{UAV} - \boldsymbol{w}_{BS} \mid^2}, \tag{1}$$

while the distance between the hybrid RIS-UAV and the user equipment is defined as:

$$d_2 = \sqrt{\mid \boldsymbol{w}_{UAV} - \boldsymbol{w}_{UE} \mid^2}. \tag{2}$$

The channels between the hybrid RIS-UAV and the ground nodes are modeled using Al-Hourani's channel model with Rician small-scale fading [10], [11]. For each channel, the probability of line-of-sight (LoS) is defined as:

$$P_{LoS}(\theta) = \frac{1}{1 + a \exp\left(-b\left[\theta - a\right]\right)}, \tag{3}$$

where a and b are constant environmental variables, and θ represents the elevation angle between the hybrid RIS-UAV and the ground nodes. Accordingly, the elevation angle between the base station and the hybrid RIS-UAV is defined as:

$$\theta_{bs} = \arctan\left(\frac{z_{UAV}}{\mid x_{UAV} - x_{BS} \mid + \mid y_{UAV} - y_{BS} \mid}\right), \tag{4}$$

while the elevation angle between the hybrid RIS-UAV and the user equipment is defined as:

$$\theta_{ue} = \arctan\left(\frac{z_{UAV}}{\mid x_{UAV} - x_{UE} \mid + \mid y_{UAV} - y_{UE} \mid}\right). \tag{5}$$

The channel gains between the base station and the hybrid RIS-UAV, and between the hybrid RIS-UAV and the user equipment, are given as [11]:

$$\mid h_{sr} \mid^2 = \frac{A \mid \Omega_{sr} \mid^2}{d_1^{\alpha_{sr}}}, \tag{6}$$

$$\mid h_{rd} \mid^2 = \frac{A \mid \Omega_{rd} \mid^2}{d_2^{\alpha_{rd}}}, \tag{7}$$

respectively. The parameter A is a constant that represents the effect of the operating frequency and is given as:

$$A = \left(\frac{4\pi f_c}{c}\right)^{-2}, \tag{8}$$

where c represents the speed of light and f_c represents the operating frequency. Besides, the parameters $\mid \Omega_{sr} \mid$ and $\mid \Omega_{rd} \mid$ shown in (6) and (7) are random variables that follow the Rician distribution and are independent and identically distributed (i.i.d). The Rician factor is defined as [12]:

$$K(\theta) = K_{min} \exp\left\{\frac{2}{\pi} \ln\left(\frac{K_{max}}{K_{min}}\right)\theta\right\}, \tag{9}$$

where K_{min} and K_{max} are the minimum and maximum Rician factor, respectively.

The aerial path loss exponents for the channels between the base station and hybrid RIS-UAV, α_{sr} and between the hybrid RIS-UAV and the user equipment, α_{rd} are defined as:

$$\alpha_{sr} = \alpha_e\left(1 - P_{LoS}(\theta_{bs})\right) + \alpha_o, \tag{10}$$

$$\alpha_{rd} = \alpha_e\left(1 - P_{LoS}(\theta_{ue})\right) + \alpha_o, \tag{11}$$

respectively, where α_e and α_o are constant variables defined by the probability of LoS [12].

For the hybrid RIS-UAV, the RIS consists of a total of N discrete elements, including L active and $N - L$ passive reflecting elements. Hence, the received signal at the user equipment is defined as:

$$y = \sqrt{P_{bs}}\mathbf{h}_{rd}^H \boldsymbol{\Psi} \mathbf{h}_{sr} s + \sqrt{P_{bs}}\mathbf{h}_{rd}^H \boldsymbol{\Phi} \mathbf{h}_{sr} s + \mathbf{h}_{rd}^H \boldsymbol{\Phi} \mathbf{n}_r + n, \tag{12}$$

where P_{bs} represents the transmit power at the base station, s represents the transmitted information signal from the base station, while $\mathbf{n}_r \sim CN\left(0, \sigma_r^2 \mathbf{I}_N\right)$ and $n \sim CN\left(0, \sigma^2\right)$ represent the thermal noise at the hybrid RIS-UAV and the user equipment, respectively. In addition, $\boldsymbol{\Psi}$ and $\boldsymbol{\Phi}$ represent the reflection matrix of the passive and active elements, respectively, where $\boldsymbol{\Psi} = \text{diag}\left\{\Psi_1, \ldots, \Psi_N\right\}$ and $\Phi = \text{diag}\left\{\Phi_1, \ldots, \Phi_N\right\}$,

$$\Psi_n = \begin{cases} 0, & n \in \mathbb{L} \\ e^{j\varphi_n}, & otherwise \end{cases}, \tag{13}$$

$$\Phi_n = \begin{cases} \rho_n e^{j\varphi_n}, & n \in \mathbb{L} \\ 0, & otherwise \end{cases}. \tag{14}$$

The positions of L active elements are denoted as $\mathbb{L} \subset \{1, 2, \cdots, N\}$, and the phase shift of the n-th element is denoted as φ_n, such that $\varphi_n \in [0, 2\pi]$. For simplicity, the amplification gain is identical, i.e., $\rho_n = \rho$ for all active elements.

In the scenario of assuming the ideal phase-shifting case, the signal-to-noise ratio (SNR) for the hybrid RIS-UAV is defined as:

$$\gamma = \frac{P_{bs}\left((N-L)^2 \mid h_{sr} \mid^2 \mid h_{rd} \mid^2 + \rho^2 L^2 \mid h_{sr} \mid^2 \mid h_{rd} \mid^2\right)}{\rho^2 \sigma_r^2 L \mid h_{rd} \mid^2 + \sigma^2}, \tag{15}$$

while the achievable rate of the system is given as:

$$R = B \log_2 (1 + \gamma), \tag{16}$$

where B represents the system bandwidth.

A. Achievable Rate Maximization Problem

In this paper, the UAV's altitude, amplification gain of the active RIS elements, transmit power allocation at the BS and hybrid RIS are optimised to maximise the achievable rate of the system. Given the total power budget, P_{total} for supplying the hardware power and the signal transmission, such that [13]:

$$P_{total} = \underbrace{P_{hard\_bs} + P_{hard\_ue} + NP_{sw} + LP_{dc}}_{P_{hardware}} + \underbrace{P_{bs} + P_{ris}}_{P_{comm}}, \tag{17}$$

where P_{hard_bs} and P_{hard_ue} are the hardware-dissipated power at the base station and user equipment, respectively, while P_{sw} represents the power consumption for controlling the circuit and phase shift switch at each reflecting element, P_{dc} represents the hardware power consumption of active elements, and P_{ris} represents the transmit power at the hybrid RIS-UAV. After supplying the hardware power, $P_{hardware}$, the remaining power for signal transmission is denoted as P_{comm}.

Meanwhile, the power consumption required for the UAV to ascend to a certain altitude, z_{UAV} and maintain a hovering state for a duration of t, is denoted as P_{uav}, such that [14]:

$$P_{uav} = P_{climb}\left(\frac{z_{UAV}}{v_{climb}}\right) + (\psi + \Gamma z_{UAV})\, t, \tag{18}$$

where P_{climb} is the power required by the UAV to ascend, v_{climb} is the velocity of UAV ascending, ψ is the minimum power required for the UAV to hover above the ground, and Γ is the motor speed multiplier. Therefore, the optimisation problem is formulated as:

$$\max_{P_{bs}, P_{ris}, \rho, z_{uav}} R \tag{19}$$

$$\text{subject to } P_{bs} + P_{ris} \leqslant P_{comm} \tag{20}$$

$$P_{bs} \parallel \mathbf{\Phi}\mathbf{h}_{sr} \parallel^2 + \sigma_r^2 \parallel \mathbf{\Phi} \parallel^2 \leqslant P_{ris} \tag{21}$$

$$H_{min} \leqslant z_{UAV} \leqslant H_{max} \tag{22}$$

$$P_{climb}\left(\frac{z_{UAV}}{v_{climb}}\right) + (\psi + \Gamma z_{UAV})\, t \leqslant P_{max\_asc}, \tag{23}$$

where P_{max_asc} represents the maximum power consumption for UAV ascending. Constraint (22) is the constraint that describes the range of UAV hovering height. Since the SNR is monotonically increasing with ρ, hence the optimal ρ^2 can be computed by satisfying the condition (21):

$$\rho^2 = \frac{P_{ris}}{L\left(P_{bs} \mid h_{sr} \mid^2 + \sigma_r^2\right)}. \tag{24}$$

Thus, the SNR of the hybrid RIS-UAV with optimised ρ^2 is defined as:

$$\gamma_\rho = \frac{P_{bs}\left(P_{bs} \mid h_{sr} \mid^2 + \sigma^2\right)(N-L)^2 \mid h_{sr} \mid^2 \mid h_{rd}^2 \mid}{P_{ris}\sigma_r^2 \mid h_{rd} \mid^2 + \sigma^2\left(P_{bs} \mid h_{sr} \mid^2 + \sigma^2\right)} + \frac{P_{bs} P_{ris} L \mid h_{sr} \mid^2 \mid h_{rd} \mid^2}{P_{ris}\sigma_r^2 \mid h_{rd} \mid^2 + \sigma^2\left(P_{bs} \mid h_{sr} \mid^2 + \sigma^2\right)}, \tag{25}$$

whereas the formulated problem is simplified to:

$$\max_{P_{bs}, z_{uav}} R = B \log_2 (1 + \gamma_\rho) \tag{26}$$

subject to the constraints (20), (22), and (23).

B. Optimisation Algorithm

Genetic Algorithm (GA) is used in this paper to optimise the formulated achievable rate maximisation problem since the formulated function (25) is nonconvex concerning the z_{UAV}. Besides, GA is adopted because it guarantees the globally optimal solutions to the formulated problem. The altitude of the UAV and the transmit power at the base station are jointly optimised via iterative procedures until the achievable rate of the system, which is the cost function of the algorithm, is maximised. Generally, the GA generates a group of possible solutions, known as a population, and evolves them over multiple generations to find the optimal solution to the cost function [15]. The steps for optimising the achievable rate of the system as described below:

Step 1: Define the objective function. The cost function defined as in (26) is converted by negating it so as to minimise it using GA. So, the objective function is the negative of the cost function, and the GA is applied to search for the values of P_{bs} and z_{UAV} for minimising the objective function.

Step 2: Initialisation of the population. The GA randomly generates a group of possible solutions to the objective function, which is known as chromosomes. For a maximum of Q

generations and each generation consists of D chromosomes, the group of possible solutions at qth generation is defined as:

$$GA(q) = [\mathbf{r_1}, \ldots, \mathbf{r_d}, \ldots, \mathbf{r_D}]^T, \quad (27)$$

where $[.]^T$ represents the transpose operator, and $\mathbf{r_d}$ represents the structured chromosome with randomly generated values of P_{bs} and z_{UAV} such that the constraints (20), (22), and (23) are satisfied.

Step 3: Evaluation of the fitness. The fitness of each possible solution is evaluated by computing the objective function value for each value of P_{bs} and z_{UAV}.

Step 4: Selection of the parents. The fittest chromosomes are selected to be the parents of the next generation.

Step 5: Crossover and Mutation. The selected parents are then combined to form the offspring of the next generation, and the offspring are mutated randomly to create new genetic materials for the population.

Step 6: Iterative process. The new population generated is used to replace the current population, and steps 3 to 5 are repeated until the termination condition is met, such that the maximum number of iterations is reached.

Step 7: Termination and return the solution. The obtained solution, which corresponds to the values of the UAV's altitude and the transmit power at the base station that minimises the objective function, is then converted by negating it to maximise the original cost function.

III. Results and Discussions

In this section, numerical results are presented to evaluate the performance of hybrid RIS-UAV by optimising the UAV's altitude, transmit power allocation at the base station and hybrid RIS. All the results are obtained through Monte Carlo simulations, and the simulation parameters used are listed in Table 1 [12]–[14]. For the position of the ground nodes, the coordinates of the base station and user equipment are fixed at $(0, 0, 0)$ and $(100, 0, 0)$, respectively. Whereas, the default position of the UAV is hovering at coordinate (90,0,20). In addition, the environmental parameters are based on dense urban scenarios.

As shown in Fig. 2, the conventional fully-passive RIS-UAV suffers from the double path-loss problem, especially when the RIS-UAV is situated at a considerable distance away from both the base station and the user equipment. On the other hand, hybrid RIS-UAV overcomes the double path-loss problem while boosting the signal strength with the amplification factor. With a single active element, the hybrid RIS-UAV achieves about 14 times higher rate than the fully-passive RIS-UAV when the RIS-UAV is placed at the centre between the base station and user equipment.

By optimising the transmit power at the base station and the hybrid RIS-UAV, the achievable rate of the hybrid RIS-UAV improved by 10% and 15% when the hybrid RIS-UAV is situated near the base station and user equipment, respectively. When the hybrid RIS-UAV is positioned at the midpoint between the base station and user equipment, equal power allocation is optimal due to the symmetry in the distances and channel characteristics for both channel links, from the base station to the hybrid RIS-UAV and from the hybrid RIS-UAV to the user equipment. Therefore, the achievable rate of the power-optimised hybrid RIS-UAV matches that of the unoptimised case, as both allocate power equally between the base station and the hybrid RIS-UAV. However, by optimising the UAV's altitude, the achievable rate of the hybrid RIS-UAV is 1.94 times higher than the unoptimised case, as stronger LoS links between the hybrid RIS-UAV and the ground nodes improve the channel gain and SNR of the received signals. Moreover, the achievable rate of the hybrid RIS-UAV is further improved by 4.3% once the UAV's altitude and power allocation are jointly optimised. Compared to the conventional fully-passive RIS-UAV, the joint-optimised hybrid RIS-UAV outperforms it by 22 times when the RIS-UAV is placed at

TABLE I
Simulation Parameters

Parameter	Default Value
α_e; α_o	1.5; 2
a; b	11.95; 0.136
K_{min}; K_{max}	5 dB; 15 dB
H_{min}; H_{max}	5; 120
N; L	256; 1
f_c	2.3 GHz
B	10 MHz
σ_r^2;σ^2	-90 dBm
P_{sw}	-10 dBm
P_{dc}	-5 dBm
P_{hard_bs}; P_{hard_ue}	10 dBm
P_{total}	30 dBm
P_{climb}	85 $watts$
v_{climb}	2 m/s
ψ	30
Γ	10.5
t	1200 $seconds$
P_{uav}	$1x10^6$ $watts$

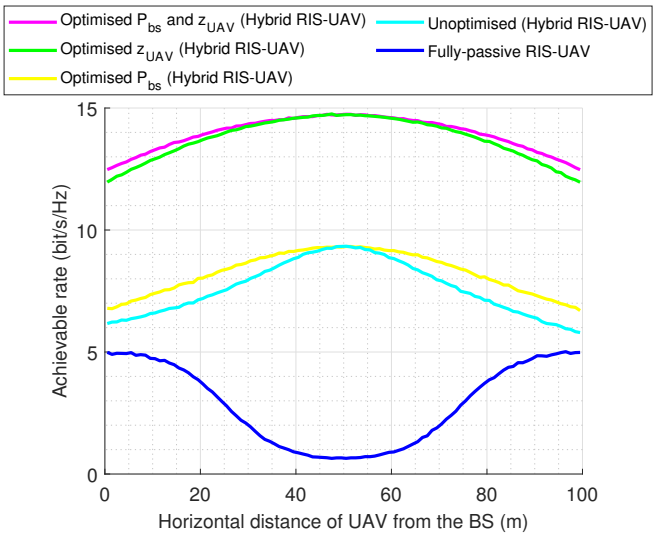

Fig. 2. Achievable rate of the RIS-UAV versus the horizontal distance of UAV from the base station.

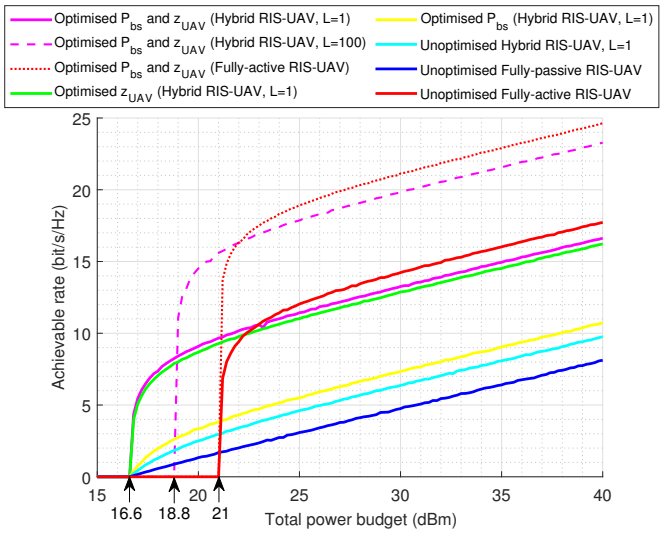

Fig. 3. Achievable rate of the RIS-UAV versus the total power budget.

the centre point between the base station and user equipment.

Meanwhile, Fig. 3 shows that a larger power budget is required by the fully-active RIS-UAV to supply the hardware power compared to the hybrid and passive RIS-UAV. In other words, passive RIS-UAV can operate at a lower power budget, such that the power budget required is only 16.6 dBm while active RIS-UAV requires 21 dBm in order to supply the hardware components of the elements. For the hybrid RIS-UAV, a power budget of 16.6 dBm and 18.8 dBm is required if the number of active elements is one and 100, respectively. Since the SNR of the RIS-UAV is an increasing function of L, hence the achievable rate increases with the number of active elements, but a higher power budget is required.

For the joint-optimised hybrid RIS-UAV, better performance can be achieved by increasing the number of active elements, such that the achievable rate is increased by about 50% with 100 active elements. By jointly optimising the UAV's altitude, transmit power allocation at the base station and hybrid RIS, the achievable rate of the hybrid RIS-UAV with 100 active elements outperforms the unoptimised fully-active RIS-UAV even though the number of active elements of the latter is higher than the former. When the UAV's altitude, transmit power allocation at the base station and hybrid RIS of the fully-active RIS-UAV are jointly optimised, the achievable rate can be improved by 57% compared to the unoptimised fully-active RIS-UAV. The optimal number of active elements for the hybrid RIS-UAV is a potential future work to improve the system performance while maintaining low power consumption.

IV. Conclusions

The integration of RIS and UAV has emerged as a promising solution for the future wireless communication network. Therefore, this paper investigated the achievable rate maximisation problem of the hybrid RIS-UAV system, in which the RIS that is mounted on the UAV consists of both active and passive elements. The optimisation parameters include the UAV's altitude, transmit power allocation at the base station and hybrid RIS. Based on the results simulated, the joint-optimised hybrid RIS-UAV achieves a rate improvement of twice the unoptimised hybrid RIS-UAV. In addition, the joint-optimised hybrid RIS-UAV outperforms the conventional passive RIS-UAV by 22 times in terms of the achievable rate. Hence, the application of hybrid RIS-UAV in assisting the ground communication system is promising for improving wireless communication.

Acknowledgment

This work was supported by Universiti Teknologi Malaysia under Grant 22H33, in part by the Ministry of Higher Education Malaysia through the Higher Institution Centre of Excellence (HICOE) Grant 4J636 and in part by H2020-MSCA-RISE-2020 under Grant 101008085.

References

[1] Q. Wu, S. Zhang, B. Zheng, C. You, and R. Zhang, "Intelligent reflecting surface-aided wireless communications: A tutorial," IEEE Transactions on Communications, vol. 69, pp. 3313–3351, 2021.

[2] A. C. Pogaku, D.-T. Do, B. M. Lee, and N. D. Nguyen, "Uav-assisted ris for future wireless communications: A survey on optimization and performance analysis," IEEE Access, vol. 10, pp. 16 320–16 336, 2022.

[3] K.-W. Park, H. M. Kim, and O.-S. Shin, "A survey on intelligent-reflecting-surface-assisted uav communications," Energies, vol. 15, no. 14, p. 5143, Jul 2022.

[4] M. Munochiveyi, A. C. Pogaku, D. Do, A. Le, M. Voznák, and N. D. Nguyen, "Reconfigurable intelligent surface aided multi-user communications: State-of-the-art techniques and open issues," IEEE Access, vol. 9, pp. 118 584– 118 605, 2021.

[5] C.Y. Goh, C.Y. Leow, and R. Nordin, "Energy efficiency of unmanned aerial vehicle with reconfigurable intelligent surfaces: a comparative study," Drones, vol. 7, no. 2, pp. 98, 2023.

[6] X. Pang, M. Sheng, N. Zhao, J. Tang, D. Niyato, and K. Wong, "When uav meets irs: expanding air-ground networks via passive reflection," IEEE Wireless Communications, vol. 28, no. 5, pp. 164–170, 2021.

[7] D. Wang, Y. Zhao, Y. He, X. Tang, L. Li, R. Zhang, and D. Zhai, "Passive beamforming and trajectory optimization for reconfigurable intelligent surface-assisted uav secure communication," Remote Sensing, vol. 13, no. 21, p. 4286, 2021.

[8] T. Shafique, H. Tabassum, and E. Hossain, "Optimization of wireless relaying with flexible uav-borne reflecting surfaces," IEEE Transactions on Communications, vol. 69, no. 1, pp. 309–325, 2021.

[9] N. T. Nguyen, Q.-D. Vu, K. Lee, and M. Juntti, "Hybrid relay-reflecting intelligent surface-assisted wireless communications," IEEE Transactions on Vehicular Technology, vol. 71, pp. 6228–6244, 2022.

[10] A. Al-Hourani, S. Kandeepan, and S. Lardner, "Optimal lap altitude for maximum coverage," IEEE Wireless Communications Letters, vol. 3, pp. 569– 572, 2014.

[11] M. M. Azari, F. Rosas, K.-C. Chen, and S. Pollin, "Ultra reliable uav communication using altitude and cooperation diversity," IEEE Transactions on Communications, vol. 66, pp. 330–344, 2018.

[12] W. K. New, C. Y. Leow, K. Navaie, and Z. Ding, "Robust non-orthogonal multiple access for aerial and ground users," IEEE Transactions on Wireless Communications, vol. 19, pp. 4793–4805, 2020.

[13] K. Zhi, C. Pan, H. Ren, K. K. Chai, and M. Elkashlan, "Active ris versus passive ris: which is superior with the same power budget?" IEEE Communications Letters, vol. 26, no. 5, pp. 1150–1154, 2022.

[14] M. F. Sohail, C. Y. Leow and S. Won, "Energy-efficient non-orthogonal multiple access for uav communication system," in IEEE Transactions on Vehicular Technology, vol. 68, no. 11, pp. 10834-10845, Nov. 2019.

[15] S. Jayaprakasam, S. K. A. Rahim, and C. Y. Leow, "A pareto elite selection genetic algorithm for random antenna array beamforming with low sidelobe level", Progress In Electromagnetics Research B, vol. 51, 407-425, 2013.